1-1-2006

Endocytosis of cadherin from intracellular junctions is the driving force for cadherin adhesive dimer disassembly

Regina B. Troyanovsky
Washington University School of Medicine in St. Louis

Eugene P. Sokolov
Washington University School of Medicine in St. Louis

Sergey M. Troyanovsky
Washington University School of Medicine in St. Louis

Molecular Biology of the Cell
Vol. 17, 3484–3493, August 2006

Endocytosis of Cadherin from Intracellular Junctions Is the Driving Force for Cadherin Adhesive Dimer Disassembly

Regina B. Troyanovsky, Eugene P. Sokolov,* and Sergey M. Troyanovsky

Division of Dermatology, Washington University Medical School, St. Louis, MO 63110

Submitted March 13, 2006; Revised May 12, 2006; Accepted May 31, 2006
Monitoring Editor: Asma Nusrat

The adhesion receptor E-cadherin maintains cell–cell junctions by continuously forming short-lived adhesive dimers. Here mixed culture cross-linking and coimmunoprecipitation assays were used to determine the dynamics of adhesive dimer assembly. We showed that the amount of these dimers increased dramatically minutes after the inhibition of endocytosis by ATP depletion or by hypertonic sucrose. This increase was accompanied by the efficient recruitment of E-cadherin into adherens junctions. After 10 min, when the adhesive dimer amount had reached a plateau, the assembly of new dimers stalled completely. These cells, in a striking difference from the control, became unable to disintegrate both their intercellular contacts and adhesive dimers in response to calcium depletion. The same effects, but after a slightly longer time course, were obtained using acidic media, another potent approach inhibiting endocytosis. These data suggest that endocytosis is the main pathway for the dissociation of E-cadherin adhesive dimers. Its inhibition blocks the replenishment of the monomeric cadherin pool, thereby inhibiting new dimer formation. This suggestion has been corroborated by immunoelectron microscopy, which revealed cadherin-enriched coated pit-like structures in close association with adherens junctions.

INTRODUCTION

Classic cadherins are transmembrane adhesion receptors that mediate Ca^{2+}-dependent cell–cell adhesion within adherens junctions in many types of cells. It is widely accepted that extracellular cadherin regions establish a direct connection between two opposing plasma membranes through trans homodimerization. Clusters of such cadherin complexes constitute the adhesion transmembrane core of the adherens junctions. Catenins, the proteins interacting with the cadherin intracellular domain, couple these clusters either directly or indirectly to the cortical cytoskeleton (Provost and Rimm, 1999; Gumbiner, 2005; Nelson *et al.,* 2005). Although cadherin-mediated adhesion is very important for various normal and abnormal morphogenetic events, little is clear beyond this very general model.

A key event in adherens junction assembly is the adhesive cadherin–cadherin interaction. The molecular details of this important process make up the most controversial issue of cadherin-based adhesion (reviewed in Leckband and Sivasankar, 2000; Patel *et al.,* 2003; Troyanovsky, 2005). Using two different strategies—coimmunoprecipitation and site-specific cross-linking assays—we have revealed adhesive and lateral E-cadherin homodimers (Troyanovsky, 2005). One of the notable features of these complexes is their stability; once extracted from the cells, the dimers are stable in SDS concentrations as high as 0.2%, regardless of the presence of calcium ions. The assembly of cadherin dimers stable enough to sustain cell solubilization and an ensuing coimmunoprecipitation procedure has also been documented by others (Shan *et al.,* 2000; Ozawa, 2002). This feature of cadherin dimers indicates the high affinity of the corresponding cadherin–cadherin interactions. Molecular analysis of adhesive and lateral dimers (Laur *et al.,* 2002; Troyanovsky *et al.,* 2003) implied that they both correspond to the strand cadherin dimer, a dimer in which the Trp156 residue of each molecule reciprocally inserts into a pocket of the paired molecule (Shapiro *et al.,* 1995; Boggon *et al.,* 2002). Initially such an interaction had been proposed to establish lateral dimers (Shapiro *et al.,* 1995), but a subsequent crystallographic study of C-cadherin suggested the role of this interaction in the formation of adhesive bonds (Boggon *et al.,* 2002).

Cell–cell adhesion structures are not static. Live imaging of GFP-tagged E-cadherin has demonstrated continuous remodeling of adherens junctions (Adams *et al.,* 1998). The high dynamics of adherens junctions have been proposed to be based on low-affinity adhesive intercadherin interactions (Kusumi *et al.,* 1999). By this hypothesis, the initial contact between two plasma membranes triggers two local processes, cadherin clustering and the anchorage of cadherin clusters to the cortical cytoskeleton. Cadherin clusters stabilize the weak adhesive bonds of individual cadherin molecules. Cells are proposed to form and disintegrate adhesive contacts using the cytoskeleton, which mediates cadherin clustering. Thus, according to this "traditional" model of cadherin-based adhesion, weak cadherin–cadherin interaction is a critical element essential for the remarkable plasticity of adherens junctions.

If, however, cell–cell adhesion is based on strong cadherin–cadherin interactions, a remodeling of adherens junctions requires completely different mechanisms. By our hypothesis, cadherin adhesion is mediated by the continuous formation of short-lived adhesive dimers within cell–cell junctions (Troyanovsky, 2005). Indeed, our work has shown that un-

This article was published online ahead of print in *MBC in Press* (http://www.molbiolcell.org/cgi/doi/10.1091/mbc.E06–03–0190) on June 7, 2006.

* Present address: Biology Department, University of North Carolina at Charlotte, Charlotte, NC 28223.

Address correspondence to: Sergey Troyanovsky (sergeyt@im.wustl.edu).

der standard culture conditions the lifetime of cadherin dimers lasts only a few minutes (Klingelhofer *et al.*, 2002). The short lifetime of cadherin dimers in vivo and their high stability in vitro suggest that a specific cellular mechanism is required for the continuous dissociation of cadherin dimers in intracellular contacts. In this case the adhesive contact, its strength, and its plasticity would be regulated by an equilibrium between two opposing processes: adhesive dimer assembly and disassembly.

In this work we investigate the mechanisms responsible for cadherin dimer instability in vivo. We show that cadherin dimers are markedly stabilized in A-431 epithelial cells upon ATP depletion or the inhibition of endocytosis by hypertonic sucrose or acidic media. The blockage of cadherin dimer dissociation results in a sharp increase in the total amount of adhesive dimers and a concomitant depletion of the cadherin monomeric pool. Fully supporting the role of endocytosis in adhesive dimer dissociation, our immunoelectron microscopy of A-431 and HaCaT epithelial cells revealed numerous E-cadherin–containing endocytic invaginations closely associated with adherens junctions.

MATERIALS AND METHODS

Cell Culture and Antibodies

Transfection, growth, and immunofluorescence microscopy of human A-431 cells were done as described (Chitaev and Troyanovsky, 1998). A-431 cell subclones expressing E-cadherin (or its mutants) tagged either by myc (Ec1M) or by flag (Ec1F) epitopes and lacking the epitope for C20820 monoclonal antibody were described (Chitaev and Troyanovsky, 1998). The following antibodies were used: anti-E-cadherin, clones HECD-1 (Zymed Laboratories, South San Francisco, CA) and C20820 (Transduction Laboratories, Lexington, KY), anti-myc (clone 9E10), and anti-flag M2 (Sigma, St. Louis, MO).

Plasmids

The plasmids coding for the new cysteine mutants Ec1M-C163A/T227C (for simplicity Ec227M) and Ec1F-C163A/W213C (Ec213F) were constructed using site-directed mutagenesis in the expression vector pRcCMV (Invitrogen, Carlsbad, CA). To design these mutants the model of the N-cadherin EC1 domain strand dimer (Protein Data Bank ID code 1NCI) was used. Molecular structures were analyzed using RasMol2 and Cn3D4.1 programs. Correct plasmid construction was verified by endonuclease mapping and nucleotide sequencing.

Mixed Culture Coimmunoprecipitation Assay

The mixed culture coimmunoprecipitation assay has previously been described (Chitaev and Troyanovsky, 1998). In brief, equal amounts of A-431 cells producing myc- and flag-tagged forms of E-cadherin (Ec1M and Ec1F, respectively) were mixed and cultured for 24 h. Cells were extracted with 1.5 ml of IP-buffer (50 mM Tris-HCl, pH 7.4, 150 mM NaCl, 0.5 mM AEBSF, 2 mM EDTA, and 1% NP-40). NP-40–insoluble material was removed by centrifugation at 100,000× *g* for 1 h. The lysates were subjected to immunoprecipitation by subsequent incubations with anti-myc antibody and protein A-Sepharose. In this assay anti-myc antibody coimmunoprecipitates Ec1F, which can be derived only from adhesive Ec1M-Ec1F dimers.

In some experiments the actin filament inhibitors, such as cytochalasin D (Sigma; final concentration, 5 μM), latrunculin A (Molecular Probes, Eugene, OR; 0.2 μM), Y-27632, or ML-7 (both Calbiochem, La Jolla, CA; final concentration 10 and 15 μM, respectively) were added to the culture medium for 30 min at 37°C before cell lysis. To inhibit endocytosis, cells were incubated for various times with a culture medium containing 0.4 M sucrose at 37°C (Heuser and Anderson, 1989) or with acidic (pH 5.5) media (Heuser, 1989). Depletion of ATP was achieved by using a combination of glycolytic (2-deoxy-D-glucose) and oxidative (antimycin A or NaN_3) inhibitors, as described previously (Shelden *et al.*, 2002). In brief, A-431 monolayers were rinsed with HEPES-buffered saline (HBS; 20 mM HEPES, 135 mM NaCl, 4 mM KCl, 1 mM Na_2HPO_4, 2 mM $CaCl_2$, 1 mM $MgCl_2$, pH 7.2) and then exposed to ATP depletion medium (HBS containing 2 mM 2-deoxy-D-glucose and 1 μM antimycin A or 5 mM NaN_3) for the times indicated. Where conditions are indicated as low calcium, the buffers or media contained 20 μM calcium instead of 2 mM.

Cross-linking Assays

The homobifunctional chemical cysteine-specific cross-linkers BM[PEO]3 or DPDPB (Pierce, Rockford, IL) containing different cysteine-reactive groups, were used for cell surface protein cross-linking. Confluent cultures were washed with phosphate-buffered saline (PBS) containing 0.5 mM $CaCl_2$ (PBS-C). Each plate was then incubated for 10 min at room temperature in PBS-C containing 1 mg/ml cross-linker. The reaction was stopped by washing the cells with PBS containing, in case of BM[PEO]3, 2 mM DTT. Surface-cross-linked cells were solubilized directly in the SDS gel sample buffer and the extracts were separated by 5% SDS-PAGE and analyzed by immunoblotting as described (Troyanovsky *et al.*, 2003).

In some experiments cell surface proteins were biotinylated with EZ-link PEO-Maleimide-Activated Biotin (Pierce) after DPDPB cross-linking. Cells were washed first with PBS-C with 1 mM cysteine, followed by two washes with PBS-C, and then incubated for 20 min at 4°C with a biotinylation reagent that has been solubilized in PBS-C immediately before use. Then cells were immunoprecipitated with the anti-myc antibody as described above. Biotinylated proteins were visualized with streptavidin-HRP conjugate.

For the mixed culture cross-linking assay, cells expressing Ec227M mutant (A227M cells) were mixed in a 1:3 ratio with cells expressing Ec213F and were cross-linked a day later as described above. To analyze the dimerization dynamics, cells were plated at the same 1:3 ratio in one row (8 wells) of the 48-well plates. On the next day the cell-containing wells were washed with cold HBS buffer, pulse-labeled with a cross-linker at concentration 50 μg/ml for 30 s at room temperature (RT), washed twice with cold HBS, and chased in cysteine/serum-free culture medium at 37°C for up to 10 min. At the end of chase periods, the cells were lysed in a DTT-free SDS-sample buffer. All manipulations were synchronized using multichannel pipettors. In some cases cells before pulse-labeling were treaded for 2 min with 0.05% digitonin (in calcium-free HBS).

Trypsin-based Dissociation Assay

This assay is a slight modification of the dispase-based dissociation assay described by Huen *et al.* (2002). Confluent 3-d-old cultures of A-431 cells on 60-mm dishes were washed twice in HBS and then incubated in 4 ml of HBS with 0.01% trypsin for 20 min at 37°C. Before trypsin treatment, some plates were preincubated for 10 min either with metabolic inhibitors or hypertonic sucrose as indicated above. The same inhibitors were added to all solutions destined for the corresponding plates. Epithelial sheets, which were released from the cell substrate by trypsin, were carefully washed twice in HBS containing 10% fetal calf serum (FCS) (HBS-fetal calf serum) and soybean trypsin inhibitor (10 μg/ml). Then, the plates were washed by HBS-fetal calf serum containing 4 mM EDTA instead of calcium ions and were shaken (100 rpm, 37°C) in the same EDTA-containing buffer (3 ml) for 20 min. Resulting cell suspensions were analyzed using an inverted microscope.

Internalization Assay

The overall rate of E-cadherin endocytosis was determined essentially as described (Le *et al.*, 1999). In brief, cells were surface-biotinylated using sulfo-NHS-SS-biotin (Pierce; 1 mg/ml, for 10 min at 4°C), followed by washing with 50 mM NH_4Cl (in PBS-C). The cells were then incubated in normal medium (37°C) for various durations to resume endocytosis. Noninternalized biotin was then stripped from the surface by two 20-min washes with glutathione solution (50 mM in 90 mM NaCl, 1 mM $MgCl_2$, 0.1 mM $CaCl_2$, 60 mM NaOH, 1% FCS at 0°C). The internalized biotinylated proteins were precipitated by streptavidin-agarose (Sigma) and analyzed by immunoblotting.

Electron Microscopy

For conventional electron microscopy (EM), aclar cover slips with confluent cells were fixed for 1 h with 4% formaldehyde/0.5% glutaraldehyde in PBS, then washed with 100 mM phosphate buffer, and fixed in 1% osmium tetroxide (Polysciences, Warminster, PA) in 100 mM phosphate for 30 min at RT. The samples were then rinsed extensively in deionized water and stained with 1% aqueous uranyl acetate (Ted Pella, Irvine, CA) for 20 min at RT. After staining, the samples were again rinsed in water, dehydrated in a graded series of ethanol, and embedded in Eponate 12 resin (Ted Pella). Sections of 70–80 nm were cut, stained with uranyl acetate and lead citrate, and viewed on a JEOL 1200 EX transmission electron microscope (Peabody, MA).

Pre-embedding immuno-EM was adapted from Laube *et al.* (1996). Coverslips were fixed as above. Free aldehyde groups were blocked by 5-min incubation in PBS with 0.02 M glycine. Then, cells were incubated with HECD-1 antibody for 1 h (in PBS supplemented with 0.05% BSA), washed in PBS, and incubated for 1 h with ultrasmall gold-conjugated Fab′ fragments of the goat anti-mouse IgG (Nanoprobes, Yaphank, NY). After the gold particles had bound, the samples were washed three times for 5 min with PBS and fixed for 15 min with 1% glutaraldehyde (in PBS) and again washed in PBS and then in deionized water. The size of the gold particles was enhanced using the HQ silver enhancement kit (Nanoprobes) with one 5-min cycle. For light microscopy an additional 5-min cycle was added. The reaction was stopped by rinsing with deionized water, followed by gold toning, which consisted of a10-min incubation with gold chloride (Sigma) in 150 mM acetate buffer (pH 5.3), a short rinse with 150 mM acetate buffer, and a 10-min fixation in 0.1 M sodium thiosulfate in 20 mM HEPES (pH 7.4). After gold toning, samples were processed as indicated above for conventional EM.

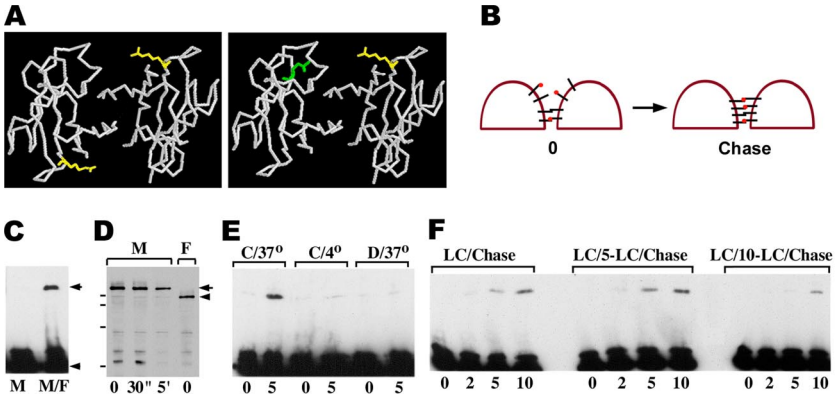

Figure 1. (A) The backbone structure of N-cadherin EC1 domain strand dimer according to Shapiro *et al.* (1995), as viewed from the carboxyl-termini. The side chains of the residues corresponding to E-cadherin T^{227} (yellow) and W^{213} (green) are shown. Left panel, cysteines, when occupy the T^{227} position, are located at the opposite sides of the strand dimer that makes their cross-linking difficult. In contrast, the heterodimer consisting of T227C and W213C mutants (right panel) exposes two closely opposed cysteines. (B) Schematic representation of our experiment. Brief treatment of the A227M/A213F coculture with the cysteine-specific cross-linker (red dots) should cross-link a low amount of adhesive dimers and interact via one reactive group with some fraction of the monomeric Ec227M and Ec213F mutants (left panel, *0*). The subsequent adhesive dimerization of so-labeled mutants with their unlabeled counterparts would result in the cross-linking reaction (right panel). (C) Homogeneous culture of A227M cells (lane M) and a mixed culture of A227M and A213F cells (lane M/F) were cross-linked by BM[PEO]3 (1 mg/ml, 5 min at RT). Their total lysates were analyzed by Western blotting with anti-myc antibody. Note that cross-linked dimers (arrow) are produced only in coculture. Monomeric form is indicated by arrowhead. (D) A227M and A213F cells (lanes M and F, respectively) were first labeled with the cysteine-specific cross-linker DPDPB (50 μg/ml, RT; times of labeling are indicated under corresponding lanes). Residual unlabeled cysteines were then biotinylated by maleimide-biotin surface labeling. Western blot was developed using streptavidin-peroxidase. Myc- and flag-tagged mutants are indicated by the arrow and arrowhead, respectively. Note that E-cadherin mutants are the predominant biotinylated proteins, and 30-s long DPDPB pulse-labeling does not notably deplete surface-exposed thiol groups. Molecular weight markers (from top to bottom: 116, 97.4, 67, and 45 kDa) are shown by horizontal bars. (E) After being DPDPB pulse-labeled (50 μg/ml, 30 s), the A227M/A213F mixed cultures were solubilized for Western blot, either immediately (lane 0) or after 5-min chase (lane 5). Cells were chased at either 37°C (lanes C/37°) or at 4°C (lanes C/4°). Before pulse-labeling cells were pretreated with 0.05% digitonin (lanes D/37°). Note that low temperature or digitonin block the cross-linking reaction. (F) Cell–cell contacts in A227M/A213F mixed cultures were disrupted by low calcium. Cells were then DPDPB pulse-labeled and either immediately chased in a high-calcium medium (lanes LC/Chase) or the chase was applied after a 5-min (LC/5-LC/Chase) or 10-min (LC/10-LC/Chase)-long incubation in low calcium. The resulting cell lysates were analyzed by anti-myc. Chase durations in minutes are indicated below the lanes.

RESULTS

The Mixed Culture Cross-Linking Assay for Monitoring Cadherin Adhesive Dimers

In a recent work we have shown that cadherin homodimerization can be detected by cysteine-specific cross-linking of certain cadherin mutants containing Cys residues that come in close proximity to each other upon cadherin–cadherin interaction (Troyanovsky *et al.*, 2003). This approach however does not allow studying adhesive dimerization in detail because it cannot distinguish adhesive from lateral dimers. To facilitate examination of cadherin adhesive interactions, we sought to develop an approach allowing to cross-link adhesive dimers exclusively. To this end, two new E-cadherin cysteine mutants, myc-tagged Ec227M and flag-tagged Ec213F, were constructed. In these mutants, a Cys residue was introduced into position Thr227 or Trp213, respectively. According to the strand dimer model (Shapiro *et al.*, 1995; Boggon *et al.*, 2002, see Figure 1A for detail), the two Cys227 residues in the homodimers made of the Ec227M mutant are positioned too far apart to be cross-linked by cysteine-specific cross-linkers. In contrast, a heterodimer consisting of both the Ec227M and Ec213F mutants exhibits a cysteine pair compatible for cross-linking (Figure 1A, left panel).

In complete agreement with this predictions, cysteine-specific cross-linking agents BM[PE0]3 (spacer arm, 14.7 Å) or DPDPB (spacer arm, 19.9Å) were unable to cross-link Ec227M homodimers in the homogeneous culture of Ec227M-expressing A-431 cells (A227M cells, Figure 1C, lane M). However, both cross-linkers efficiently cross-linked Ec227M to the Ec213F mutant in the cocultures of A227M cells with Ec213F-expressing cells (A213F cells, Figure 1C, lane M/F). The cross-linked product could have originated only from adhesive dimers because the Ec227M and Ec213F mutants were provided by different cells.

E-Cadherin Adhesive Dimers Are Continuously Assembled

We used this new assay to study the kinetics of adhesive cadherin dimerization. Figure 1B schematically shows our experiment. Because the majority of cellular cadherin is monomeric (Klingelhofer *et al.*, 2002), the cross-linker at a low concentration should not produce a detectable amount of the cross-linked dimers. Instead it should create a small pool of the monomeric cadherin mutants coupled to only one of the two reactive groups of the cross-linker (Figure 1B, left panel). The subsequent adhesive dimerization of such "labeled" E-cadherin mutants with their corresponding unlabeled counterparts would have resulted in the cross-linking reaction (Figure 1B, right panel). Thus, an increase of the cross-linked dimers over time would reflect the kinetics of the new dimer production. To test this possibility, A227M/A213F coculture was exposed for 30 s to the cysteine-specific cross-linker DPDPB. DPDPB was selected because in contrast to BM[PEO]3, it does not produce any noticeable cross-linking of intracellular proteins (unpublished data). Biotinylation of the thiol groups that remained free after such DPDPB treatment showed that only a small pool of E-cadherin cysteine mutants reacted with DPDPB (Figure 1D). Immunoblot with anti-myc antibody verified that cells solubilized immediately after the DPDPB treatment contained only a barely detectable amount of the cross-linked Ec227M/Ec213F adhesive dimers (Figure 1E, C/37°, lane 0). However, when the DPDPB pulse-labeled cells were chased for 5 min, the amount of the Ec227M/Ec213F cross-linked dimers dramatically increased (Figure 1E, C/37°, lane 5).

To demonstrate that this increase does reflect the dynamics of adhesive dimer assembly, we performed several control experiments. First, we sought to show that the accumulation of the cross-linked product over the chase periods was not simply a result of the kinetics of the cross-linking reaction within the preexisting dimers. To this end the A227M/

A213F coculture was treated with 0.05% of digitonin before cross-linking. Such treatment does not extract cadherin adhesive dimers from the plasma membrane, but completely inactivates the dynamics of cadherin dimerization (Klingelhofer *et al.,* 2002). Figure 1E (lanes D/37°) shows that in such "stationary" conditions the yield of the cross-linked product became chase-independent. Similarly, no increase in cross-linked dimers over chase periods was revealed at 4°C (Figure 1E, lanes C/4°). Both of these control experiments indicate that the dimers cross-linked during chase periods originate from the continuous cadherin dimerization but not from the completion of the cross-linking reaction within the dimers present at time 0. This conclusion was further supported by the experiments described in detail below. They show that under certain conditions the accumulation of cross-linked dimers over the chase periods might be completely arrested.

Second, we determined for how long the DPDPB-labeled E-cadherin molecules maintain the activity of their DPDPB-derived cysteine-reactive group. The A227M/A213F cocultures were first incubated in low calcium that resulted in the complete disappearance of adhesive dimers (Chitaev and Troyanovsky, 1998). Then the cells were pulse-labeled by DPDPB and adhesive dimerization was induced (by elevating the Ca^{2+} concentration to 1 mM), either immediately or after an additional cultivation at low calcium (for 5 or 10 min). Figure 1F shows that a 5-min-long postlabeling chase in low calcium has no effect on the subsequent kinetics of adhesive dimer cross-linking. Thus, the second DPDPB reactive group remains fully active for 5 min after labeling.

Detailed analysis of the cross-linking kinetics showed that the reaction proceeded very quickly and reached a maximum in 3 min (Figure 2A). This suggests that all DPDPB-labeled molecules participate in at least one dimerization cycle in the course of 3 min. A precise assessment of the adhesive dimer lifetime is precluded, however, by several factors. We do not know 1) whether each dimerization event between the labeled and unlabeled molecules establishes a cross-link product, 2) how long a cross-linked dimer is stable, and 3) whether all or only some of the surface-exposed cadherin molecules participate in the dimerization reaction. Nevertheless, these data confirm the continual formation of adhesive dimers in A-431 cells.

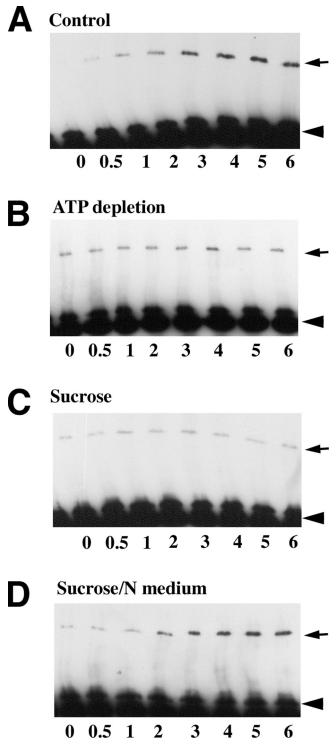

Figure 2. The kinetics of adhesive dimer assembly under various experimental conditions. A227M/A213F mixed cultures were DPDPB pulse-labeled and then chased in cysteine-free media for different time periods (indicated in min below the lanes). Total cell lysates were analyzed by anti-myc Western blotting. The arrows and arrowheads indicate cross-linked dimers and monomers, respectively. (A) Cells were chased in control media; (B) cells were depleted of ATP (for 10 min) and then were pulse-labeled and chased in the presence of metabolic inhibitors; (C) cells were pretreated with hypertonic sucrose (for 10 min) and then pulse-labeled and chased with buffers also containing hypertonic sucrose; (D) cells were pretreated and pulse-labeled in hypertonic sucrose and then chased in the regular medium. Notably, the level of the cross-linked dimers under control conditions reached a plateau within 3 min after labeling. Both ATP depletion and hypertonic media blocked the cross-linking kinetics. Normal media added to the sucrose-treated cells immediately restored adhesive dimer assembly.

ATP Depletion and Hypertonic Sucrose Arrest Dynamics of Adhesive Dimers

High stability of cadherin dimers in vitro and their dynamics in vivo suggest that cellular activity is required for adhesive dimer dissociation. The simplest explanation is that plasma membrane motions within cell–cell contacts produce physical stress leading to the continuous breaking of cadherin dimers. Because plasma membrane motion largely depends on the actin cytoskeleton, we expected that the inactivation of the actin filament function would stabilize the adhesive dimers and eventually increase their number. To test this possibility, we disrupted actin cytoskeleton by actin polymerization blockers (cytochalasin D or latrunculin A) or inhibitors of Rho kinase (Y-27632) and myosin light chain kinase (ML-7), two enzymes that also contribute to actin dynamics. The total levels of adhesive dimers in treated versus control cells were studied using a mixed culture coimmunoprecipitation assay (see Figure 3A for detail). This work showed a very modest increase in adhesive dimers after cytochalasin D treatment. Latrunculin A and Y-27632, in contrast, resulted in some reduction of cadherin dimer amounts. No changes were found after ML-7 treatment. These weak and erratic effects of anti-actin cytoskeleton drugs on cadherin dimers suggest that actin-dependent plasma membrane motion has no direct influence on the amount of cadherin dimers. We also were unable to find any effect of actin inhibitors on the kinetics of adhesive dimer assembly measured by DPDPB cross-linking of the A227M/A213F cocultures (unpublished data).

Next we asked whether ATP is required to maintain a low level of cadherin adhesive dimers. To test this idea, cellular ATP synthesis was inhibited by the oxidative phosphorylation inhibitor NaN_3 (or antimycin) in combination with the glycolysis inhibitor 2-deoxyglucose. This treatment is known to deplete cells of ATP in the course of a few minutes (Shelden *et al.,* 2002). Notably, coimmunoprecipitation experiments showed a robust assembly of adhesive dimers within 10 min of the addition of metabolic inhibitors (Figure 3B). During this period the level of the dimers reached a maximum and remained very high for up to 1 h during the subsequent treatment. In contrast, replacement of the culture medium with control buffer containing glucose produced no changes in adhesive dimer levels. ATP depletion also induced sharp changes in the adhesive dimer dynam-

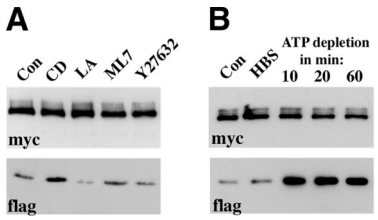

Figure 3. (A) Effects of various actin inhibitors on the total level of adhesive dimers. CD, cytochalasin D; LA, Latrunculin A; ML7, ML-7, Y27632, Y-27632; Con, control cells. Overnight AEcM/AEcF cocultures were treated by different inhibitors for 20 min and then were immunoprecipitated by an anti-myc antibody. The blots were probed for the presence of the immunoprecipitated Ec1M (myc) or coimmunoprecipitated Ec1F (flag). The latter could derive only from adhesive Ec1M-Ec1F dimers. (B) Effect of ATP depletion on the adhesive dimers. Overnight AEcM/AEcF cocultures were incubated in HBS buffer supplemented with glucose for 20 min (HBS), or in HBS buffer containing metabolic inhibitors for 10, 20, or 60 min (indicated above the lanes).

ics—virtually no assembly of new adhesive dimers was detected in the ATP-depleted cells during chase periods after DPDPB pulse-labeling (Figure 2B).

No significant abnormalities in A-431 cell morphology were noticed after the administration of the inhibitors. Immunomorphological examination of the control and ATP-depleted A-431 cells showed, however, pronounced changes in E-cadherin localization. In the ATP-depleted cells nearly all E-cadherin was recruited into the cell–cell contacts (Figure 4B), whereas in the control cells a large pool of this protein was found outside the contact regions (Figure 4A). Furthermore, in control cells the contact-located E-cadherin clusters (apparently representing the adherens junctions) were not prominent and E-cadherin–specific fluorescence appeared to be diffusely distributed along the cell–cell contacts. This diffused fluorescence was markedly reduced in the ATP-depleted cells.

Taken together, these data showed that the dissociation of E-cadherin adhesive dimers is an ATP-dependent active process. Inhibition of this process leads to the rapid accumulation of adhesive dimers within the junctions, concomitantly reducing the pool of monomeric cadherin available for new dimer assembly. The well-known energy-dependent process that could potentially disrupt adhesive dimers is E-cadherin endocytosis, which had been shown to mediate cadherin recycling in epithelial cells (Le *et al.,* 1999). To test if endocytosis is, indeed, required for adhesive dimer dissociation, we studied cadherin dimer dynamics in cells in which endocytosis had been turned off by sucrose hypertonic shock (Heuser and Anderson, 1989). First, we confirmed that after 10 min of hypertonic sucrose, the cellular uptake of biotinylated E-cadherin was completely stopped (Figure 5A). In the same course of time, hypertonic sucrose induced a more than 10-fold increase in the amount of cadherin adhesive dimers (Figure 5B, lane sucr). After reconstitution with the isotonic medium, internalization of E-cadherin resumed immediately (Figure 5A), and the amounts of adhesive dimers returned to their normal level within 5 min (Figure 5B, lane 5).

Examination of cadherin assembly dynamics and E-cadherin cell surface distribution in cells treated with hypertonic sucrose also revealed features indistinguishable from those that were found after ATP depletion. No new cadherin dimer assembly was detected when the A227M/A213F cocultures were pretreated for 10 min in hypertonic medium

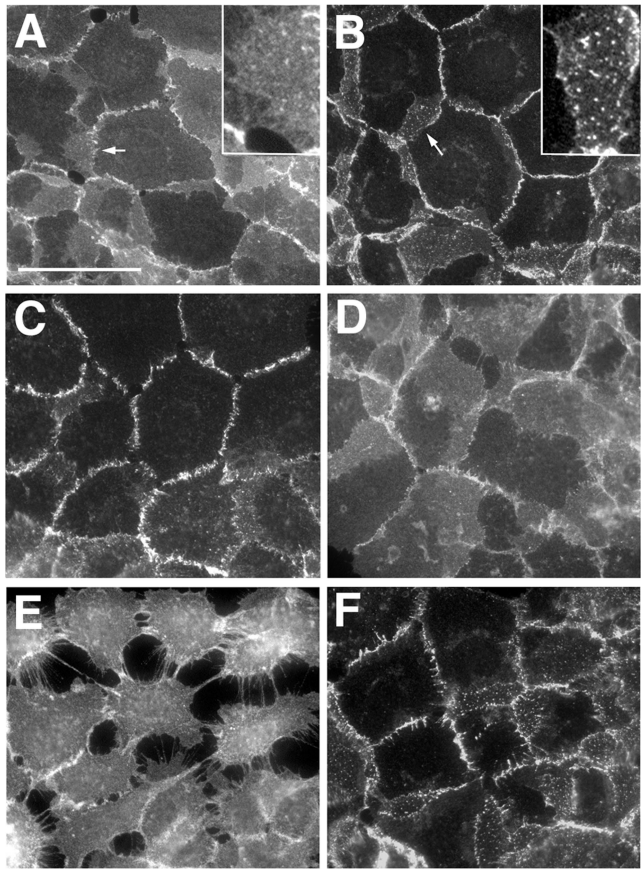

Figure 4. Immunofluorescence microscopy of wild-type A-431 cells stained with the HECD-1 anti-E-cadherin antibody. (A) Control cells. Before being fixed, the cells were (B) depleted of ATP for 10 min; (C) treated with hypertonic sucrose for 10 min; (D) treated as in C and then returned for 4 min to the regular media; (E) incubated in low calcium for 10 min; or (F) treated as in C and then transferred to the low-calcium hypertonic medium for 10 min. Higher magnifications of the selected regions (indicated by arrows) are shown in the insets. Note that hypertonic sucrose concentrated E-cadherin into the more discernible plaques and protected the cell–cell dissociation in low calcium. Bar, 50 μm.

and then were DPDPB pulse-labeled and chased also in hypertonic sucrose (Figure 2C). Isotonic medium restored the dimer dynamics within 2 min (Figure 2D). Concurrently with the stabilization of adhesive dimers, hypertonically treated cells displayed a pronounced recruitment of E-cadherin into cell–cell contact clusters and a very strong reduction of extrajunctional E-cadherin fluorescence. When cells were returned to the standard medium, these changes promptly reversed (Figure 4, C and D).

To strengthen our conclusion that cadherin internalization regulates the amount of cadherin adhesive dimers, we attempted to block endocytosis in A-431 cells by alternative protocols. However, most of them, such as potassium or cholesterol depletion and dynamin dominant-negative mutant overexpression, resulted in significant morphological abnormalities in A-431 cells that may have unspecifically affected cadherin adhesion. A 30-min-long treatment with acidic (pH 5.5) media that blocks internalization of surface proteins in many cells (Heuser, 1989) was the only alternative approach that did not alter A-431 cell morphology. Similar to hypertonic sucrose, acidic media completely

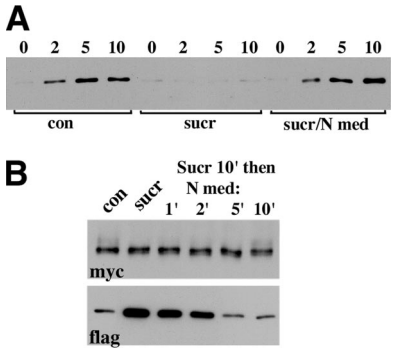

Figure 5. Effects of the hypertonic medium on E-cadherin internalization and E-cadherin adhesive dimers. (A) A-431 cells were surface-biotinylated at 4°C (lane 0), chased at 37°C (chase periods in min are indicated above the lanes), glutathione-stripped, and solubilized. Internalized proteins, which are still biotinylated, were precipitated by streptavidin beads and analyzed using an anti-E-cadherin antibody. (Con) cells were biotinylated and chased in normal conditions; (sucr) cells were preincubated (for 20 min), labeled, and chased in the hypertonic medium; (sucr/N med) cells were preincubated in the hypertonic sucrose but biotinylated and chased in the regular medium. (B) Effect of the hypertonic medium on adhesive dimers. The control AEc1M/AEc1F coculture (lane con) or after it has been treated with hypertonic sucrose (lane sucr) were analyzed by the mixed culture coimmunoprecipitation assay (see the legend for Figure 3 for detail). Note that hypertonic sucrose strongly elevated the level of adhesive dimers. When the cocultures were transferred to normal media (for 1, 2, 5, 10 min, as indicated above the lanes) after 10-min-long sucrose treatment, the amount of adhesive dimers rapidly reverted to the normal level.

blocked cadherin internalization (unpublished data). It also redistributed E-cadherin toward cell–cell contacts and dramatically increased the total amount of cadherin adhesive dimers (unpublished data). However, using this protocol we were unable to test the dynamics of cadherin dimer assembly since cysteine cross-linking is very inefficient at low pH.

Dissociation of Adhesive Dimers by Low Extracellular Calcium Is an Active Process

To produce additional evidence that endocytosis is required for the dissociation of adhesive dimers, we studied the effect of metabolic inhibitors or a hypertonic medium on the calcium dependency of cell–cell adhesion. Previously, we had shown that the removal of calcium ions from the culture medium leads to the complete disappearance of cadherin adhesive dimers. Because the dimers per se are stable at low calcium, we proposed that calcium depletion blocks the assembly of new dimers but leaves intact the disassembly process of the preexisting dimers (Klingelhofer *et al.*, 2002). If so, it is reasonable to expect that calcium removal would fail to disrupt cell–cell adhesion when the disassembly of adhesive dimers is blocked. To test this hypothesis, the control cells and cells that had been pretreated with metabolic inhibitors or hypertonic sucrose for 10 min or acidic media for 30 min were transferred to a low-calcium medium containing corresponding inhibitors. In agreement with the previous data, control cells lost cell–cell contacts (Figure 4E) and disassembled their adhesive dimers (Figure 6) in low calcium in the course of 10 min. In contrast, when cells in which cadherin endocytosis had been blocked were exposed to low-calcium medium, cell–cell contacts and E-cadherin distribution remained unchanged (Figure 4F and unpublished data). This observation is in complete agreement with recent

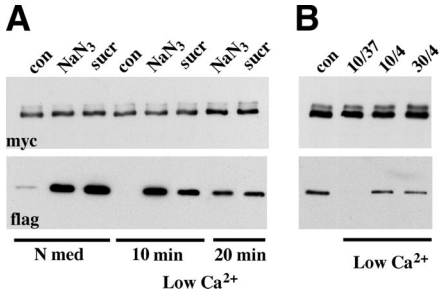

Figure 6. ATP depletion, hypertonic sucrose, and low temperature protect adhesive dimers from dissociation in low calcium. (A) The control AEc1M/AEc1F coculture (lane con) or the cocultures after a 10 min-long administration of metabolic inhibitors (lane NaN_3) or hypertonic sucrose (lane sucr) were incubated for an additional 10 or 20 min (indicated below the lanes), with the same inhibitors but at low calcium. Cell lysates were processed as indicated in Figure 3. Note that when cadherin dynamics were blocked by ATP depletion or hypertonic sucrose, a high level of adhesive dimers remained even after 20-min-long incubation with a low-calcium medium. (B) AEc1M/AEc1F cocultures were incubated in low-calcium media at 37°C for 10 min (lane 37/10), or at 4°C for 10 or for 30 min (lanes 4/10 or 4/30, respectively). Cell lysates were processed as above.

experiments reporting that hypertonic sucrose and acidic media effectively blocked disintegration of adherens junctions (Ivanov *et al.*, 2004). In addition to this, all agents preventing endocytosis that we tested (metabolic inhibitors, hypertonic sucrose, and acidic pH) also prevented dissociation of adhesive dimers in low-calcium media (Figure 6A and unpublished data). Notably, the same effect—preservation of cadherin adhesive dimers as well as cadherin subcellular distribution in low extracellular calcium—was observed when energy-dependent processes were inhibited in cells by low temperature (Figure 6B). Taken together, these data compellingly showed that dissociation of cadherin dimers in vivo results from a complex energy-dependent process.

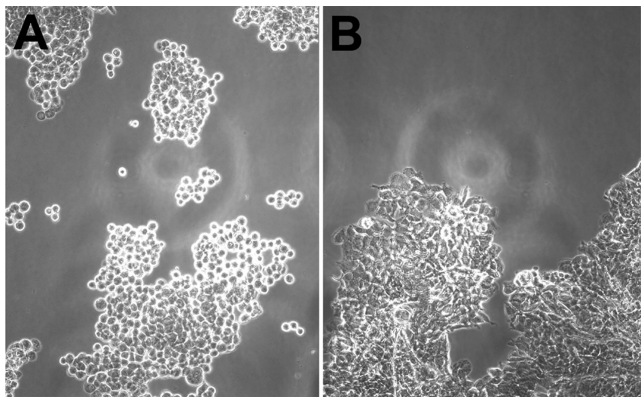

Figure 7. Hypertonic sucrose protects epithelial sheets from disintegration. Control (A) and sucrose-treated (B) monolayers were disattached from cell substrates via incubation with trypsin in the presence of calcium. After inactivation of trypsin, monolayers were transferred into EDTA-containing media and were shaken in bacterial shaker for 20 min (100 rpm at 37°C). Note that control but not sucrose-treated monolayers breakdown to small aggregates or single cells. Also note striking differences in the morphology of individual cells in the aggregates. In the control case (A) aggregates consist of loosely connected rounded cells, whereas cells are tightly packed in the case of hypertonic sucrose (B).

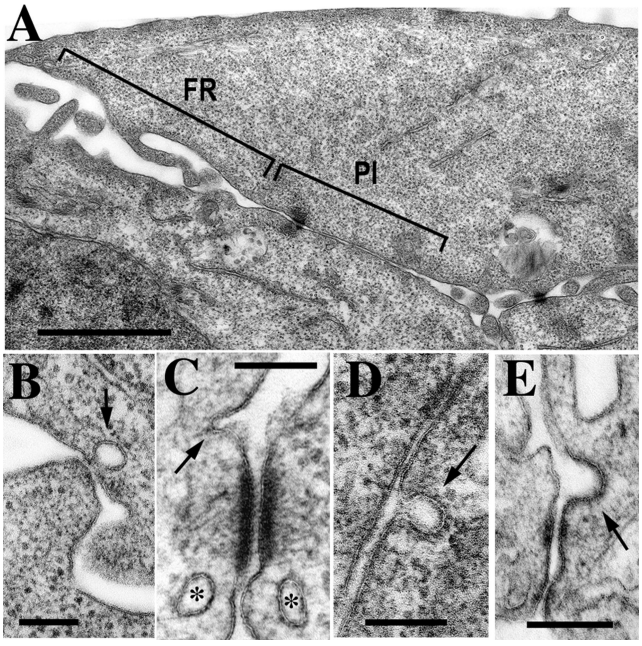

Figure 8. (A) A general view of an A-431 cell–cell interface by conventional transmission EM. The interface consists of the two morphologically distinct regions, a filopodia-reach (FR) region and a parallel interface (PI) region. Bar, 1.5 μm. (B–E) Presumptive endocytic vesicles (indicated by arrows) are frequently pinched off from various cell–cell contact junctions within both regions: at the sites of interactions with filopodia (B), in close association with a desmosome (C), or an adherens-like junction (E), or within PI region (D). Asterisks in C mark two fully formed vesicles in close proximity to the desmosome. Bars, 200 nm.

We also tested whether the inhibition of endocytosis prevents junction disruption in a trypsin-based dissociation assay. In this assay, control cell monolayers or cell monolayers after the inhibition of endocytosis (ATP-depletion and hypertonic sucrose were used for these experiments) were harvested from plates by incubation with trypsin. In the presence of calcium ions, trypsin neither affected the integrity of the monolayers nor the total amounts of cadherin or its dimers assessed by coimmunoprecipitation experiments (unpublished data). When trypsin was washed out, floating monolayers were placed into the corresponding HBS-EDTA medium. After 20 min of shaking, the cells were analyzed under inverted microscope. The differences between the two samples were obvious: the control monolayers had disintegrated completely into single cells or numerous cell aggregates consisting of only a few cells (Figure 7A). After the application of hypertonic sucrose or metabolic inhibitors, however, virtually no single cells were detected after shaking. Instead, the monolayers disintegrated into several (3–5) large fragments containing tightly connected cells (Figure 7B).

E-Cadherin Is Internalized within Adherens Junctions

To gain more evidence that dissociation of E-cadherin dimers may be mediated by endocytosis, we analyzed cell–cell contacts using EM. Conventional transmission EM showed that two morphologically different regions participate in cell–cell contact formation in A-431 cells. In the "filopodium-reach" regions (FR in Figure 8A), cells contact one another by numerous filopodia of different lengths and ~100 nm in diameter. This type of cell–cell interaction has been described for keratinocytes (Vasioukhin *et al.*, 2000). In the "parallel interface" regions (PI in Figure 8A) long stretches of the adjacent plasma membranes (up to 1 μm) are arranged in the nearly parallel manner. Both regions contain desmosomes, the hallmark of epithelial intercellular contacts. Close inspection of both regions did show a number of small endocytic invaginations in the sites of the close (<50 nm) contacts between the adjacent cells (Figure 8, B–E). The size of these structures (50–100 nm) corresponds to that of the clathrin-coated pits, whereas the absence of the well-defined electron-dense coat in these structures precludes their exact identification.

Using pre-embedding immuno-EM, we then examined whether these junction-located endocytic structures recruit E-cadherin. Because cells in these experiments were unpermeabilized, only surface E-cadherin was accessible for immunogold labeling. Figure 9A shows that at the light microscope level the immunogold anti-E-cadherin labeling was as efficient as routine immunofluorescent labeling (compare Figures 9A and 4A), indicating that the antibody readily penetrated at least into the apical regions of cell–cell contacts. EM analysis of these samples revealed that E-cadherin in the cell–cell junctions had very diverse organization. It was frequently seen as apparently individual molecules or as relatively loose and small clusters. Such regions were observed in the contacts between two filopodia or between a filopodium and a cell body (Figure 9C). These sites exhibited no submembranous electron-dense material. In the mature adherens junctions containing a typical electron dense mat of microfilaments, the clustering of gold particles was often

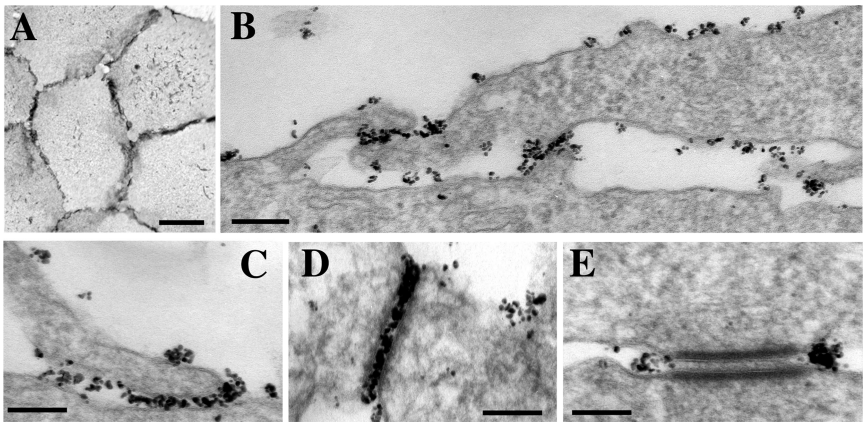

Figure 9. Anti-E-cadherin immunogold labeling of A-431 cells. The cells, which were gold-labeled, silver-enhanced, and gold-toned, were analyzed either under light microscope (A) or under EM (B–E). E-cadherin was revealed on the cell–cell junction-free cellular surface as small clusters of gold particles each of which apparently represented a single cadherin molecule. Individual E-cadherin molecules were clustered in sites of cell–cell contacts: in the sites of filopodia–cell interaction (C), in adherens junctions (D), and around desmosomes (E). Bars, 20 μm (in A), 200 nm (in B), 100 nm (in C–E).

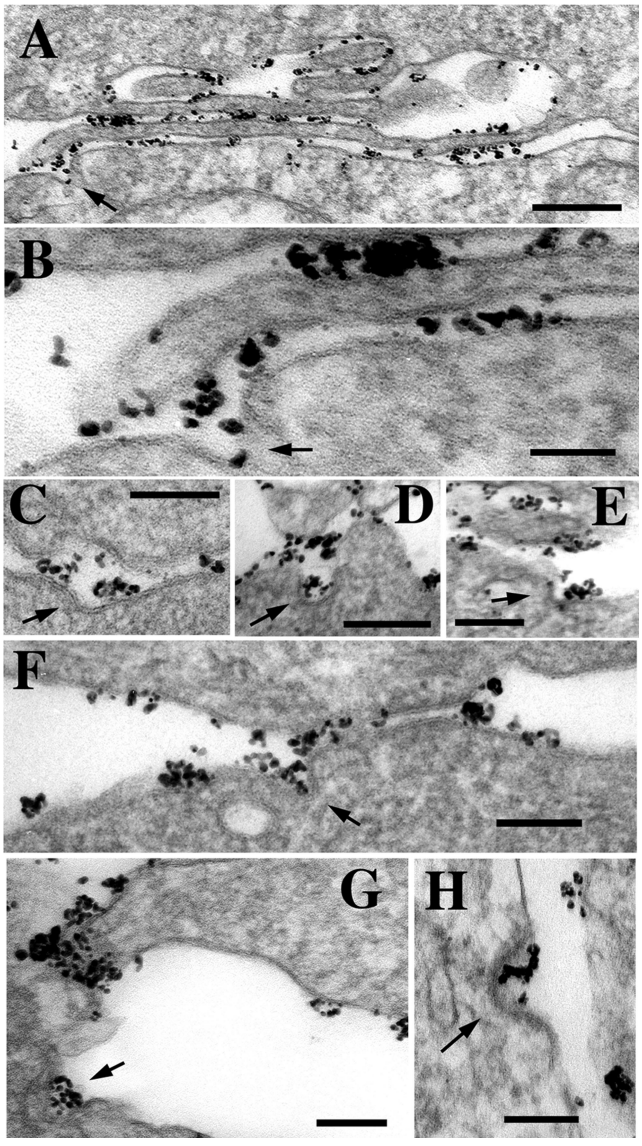

Figure 10. Anti-E-cadherin immunogold EM that detects endocytic E-cadherin–containing invaginations within various types of cell–cell junctions. (A) Low magnification (bar, 0.4 μm) of a FR region. An arrow indicates a presumptive endocytic invagination occurring in the site where a cell interacts with a tip of a filopodia. The enlargement of this site is presented in B. (C–F) Several other examples of cadherin-containing invaginations (arrows) within cadherin-containing junctions. The micrograph shown in F presents an adherens junction in HaCaT cells. (G and H) Cadherin endocytosis (arrows) was also frequently detected in cell–cell contact-free areas. Bars (B–H), 100 nm. Note that in all cases the size of invaginations is similar to that of clathrin-coated pits (100 nm), whereas only in D is the coat clearly visible.

so high that the individual particles were unresolved (Figure 9D). Furthermore, small but dense clusters of E-cadherin frequently flanked desmosomes (Figure 9E). These data demonstrate high plasticity of E-cadherin–based adhesion. In addition, a substantial pool of E-cadherin molecules was found on the apical surface of A-431 cells or on their lateral surface in the sites where the intercellular distance exceeded the possible range (~50 nm) of cadherin–cadherin adhesive bonds.

Detailed inspection of E-cadherin–stained samples presented ample evidence of E-cadherin uptake directly from cell–cell junctions. Figure 10A (and its fragment enlarged in B) shows a long filopodium adjacent to a body of the neighboring cell. The overall intercellular distance of this contact is ~30 nm, exactly corresponding to the contact in adherens junctions. At one point, the contact is interrupted from the side of the cell body by a deep E-cadherin–containing invagination (arrow). By its size and morphology this invagination is likely represent an early event of endocytosis. Three other examples of the presumed cadherin uptake from adherens junction are presented in Figure 10, C–E. In addition to the junction-associated invaginations, a number of clathrin-coated pit-like structures filled with E-cadherin were frequently seen in cell–cell interface but not in direct association with cadherin-containing junctions (Figure 10, G and H). Some invaginations showed an electron-dense coat on their cytoplasmic face (Figure 10H). On average, each cell–cell interface (~90 interfaces from 3 independent cultures were analyzed) was found to exhibit at least one example of cell–cell contact-associated or cell–cell contact-free cadherin endocytosis. To exclude a possibility that cadherin endocytosis from adherens junctions is a specific feature of A-431 cells (which are highly malignant, tumor-derived cells), we performed anti-E-cadherin gold immunolabeling of nontumorigenic HaCaT keratinocytes. Similar to A-431 cells, these cells exhibited many examples of junction-associated cadherin endocytosis (Figure 10F).

DISCUSSION

Cadherin-based cell–cell adhesion is established by homodimerization of cadherin molecules projecting from the plasma membranes of adjacent cells. Cadherin dimers potentially able to establish cell–cell adhesion were characterized in our previous work (reviewed in Troyanovsky, 2005). Only a small fraction of cadherin molecules constitutes a pool of these dimers in living cells. The rest of the molecules may exist either in the monomeric form or in multimeric complexes left undetected in the assays used in our experiments. The lifetime of the adhesive dimers apparently is very short, allowing a fast exchange between monomeric and dimeric E-cadherin pools (Klingelhofer *et al.*, 2002). In a striking difference from the in vivo data, the same dimers become remarkably stable after cell lysis. The continual turnover of adhesive dimers in vivo and their stability in vitro imply that dissociation of cadherin dimers can be an essential process regulating their total amount and thus the strength of cadherin-based adhesion.

In this work we developed a mixed culture cross-linking assay to monitoring the assembly of adhesive dimers. This assay, without determining the exact lifetime of adhesive dimers, confirmed that the dimers are very dynamic complexes. The advantage of this new assay over the one we have previously described (Klingelhofer *et al.*, 2002) is that it specifically monitors adhesive dimer dynamics without the interference of lateral cadherin dimerization. Furthermore, this assay does not include metabolic labeling, allowing one to test different pharmacological inhibitors without regard for their potential secondary effects on protein synthesis.

Using this assay we showed that the assembly of new dimers is completely blocked at 4°C and by cell permeabilization with digitonin. This clearly suggests that some cellular processes mediate dimer dynamics. One obvious candidate for such a process is the polymerization or motility of actin microfilaments associated with cadherin-containing junctions. However, neither the actin microfilament disrup-

tion (by cytochalasin D or latrunculin A) nor the inhibition of actomyosin tension (by ML-7 or Y-27632) specifically compromised both the total amount of adhesive dimers and their dynamics. Interestingly, two agents interfering with actin polymerization had opposite effects. Cytochalasin D, which blocks microfilament elongation without affecting overall F-actin contents (Cooper, 1987), resulted in an increase in adhesive dimer amounts. In contrast, this amount was reduced by latrunculin A, which completely depolymerizes actin filaments (Coue *et al.,* 1987). Such complex effect may be caused by the involvement of actin filaments in both the cadherin dimer assembly and disassembly processes. Additional work is needed to further understand the opposite outcomes of cytochalasin D and latrunculin A on the amounts of cadherin dimers.

Much more interesting and clear data were obtained with ATP inhibitors. We found that ATP depletion rapidly elevates the total level of adhesive dimers more than 10-fold. Considering that under normal culture conditions only ~5% of E-cadherin is in adhesive dimers (Klingelhofer *et al.,* 2002), this observation suggests that more than 50% of E-cadherin is converted into the dimer form in ATP-depleted cells. When the level of adhesive dimers reaches a plateau (10 min after the administration of metabolic inhibitors), formation of new dimers stalls completely. To explain this phenomenon, we proposed that ATP depletion blocks cadherin dimer dissociation, thereby preventing replenishment of the monomeric cadherin pool. Shrinking of this pool ultimately affects assembly of new cadherin dimers. Examination of cadherin dimers in cells exposed to low extracellular calcium supported such scenario. In control cells a decrease in calcium concentration results in rapid dissociation of cadherin adhesive dimers and breaking cell–cell contacts. Both dimers and contacts were resistant to low calcium when energy-dependent processes were inhibited either by ATP-depletion or low temperature.

One of many ATP-dependent mechanisms that may facilitate dimer dissociation is cadherin endocytosis. Several observations are consistent with this hypothesis. It has been shown that E-cadherin undergoes endocytosis (Le *et al.,* 1999; Akhtar and Hotchin, 2001; Lu *et al.,* 2003; Paterson *et al.,* 2003; reviewed in Bryant and Stow, 2004; Ivanov *et al.,* 2005). Inactivation of endocytosis arrests remodeling of cadherin-based junctions (Jarrett *et al.,* 2002, Palacios *et al.,* 2002). Dynamin, a protein involved in the formation of endocytotic vesicles, colocalizes with E-cadherin along the cell–cell contacts at the light microscopic level (Palacios *et al.,* 2002 and our observation; unpublished data). However, how cadherin internalization may contribute to the dissolution of adherens junctions is not clear. In particular, no studies have compellingly demonstrated the uptake of cadherin directly from adherens junctions. In contrast, recent experiments have suggested that cadherin endocytosis is limited to the extrajunctional cadherin pool and that adhesive interactions inhibit E-cadherin endocytosis, thereby stabilizing this protein at the cell surface (Izumi *et al.,* 2004).

To verify the role of cadherin endocytosis in cadherin dimer dynamics, we blocked endocytosis with hypertonic or acidic medium. Both these treatments nearly completely and reversibly arrested the endocytosis of E-cadherin (as well as transferrin and EGF receptors; unpublished data) in A-431 cells. Hypertonic sucrose, however, inhibited the uptake of cadherin much faster than acidic media (10 vs. 30 min). Like other methods known to disturb endocytosis, both of these approaches may be unspecific—though no other their targets have been reported. Similar to ATP depletion, the hypertonic medium raised the total amount of adhesive dimers more than 10-fold in 5 min. After 10 min in hypertonic media, assembly of new cadherin dimers was blocked, suggesting complete inactivation of cadherin dimer dynamics. In the same time course, a notable concentration of E-cadherin at the cell–cell contact was observed. The acidic medium produced the same effect, except this approach did not allow us to determine cadherin dimer dynamics. Furthermore, ATP depletion, hypertonic and acidic media made cell–cell adhesion calcium-independent. This was demonstrated by three groups of experiments. First, in contrast to control cells, the cells in which endocytosis had been blocked by any of three approaches, showed no changes in cadherin distribution after 20-min-long incubation in EDTA-containing medium. Calcium independence of cadherin distribution in hypertonic or acidic media was reported recently for T-84 epithelial cells (Ivanov *et al.,* 2004). Second, all agents blocking endocytosis also abolished dissociation of cadherin adhesive dimers after depletion of calcium ions. Finally, when endocytosis was inhibited, the integrity of cell–cell contacts in isolated epithelial sheets was preserved in low-calcium media even after applying shearing forces. Thus, three different experimental conditions had virtually identical effects on cadherin adhesive dimers.

Taken together these data clearly showed that the process, which is inhibited in ATP-depleted cells or in hypertonic or acidic media, is absolutely required for both the disintegration of cell–cell contacts and the dissociation of cadherin adhesive dimers. Endocytosis is the most obvious candidate for such a process; it is only one known to be inhibited in all these three conditions. However, taken into account that all inhibitors we applied are relatively unspecific, the contribution of some additional mechanisms cannot be completely excluded. For example, all these processes, in theory, might influence plasma membrane permeability or other basic membrane properties. Furthermore, because all these conditions prevent the internalization of nearly all surface proteins, it is possible that the internalization of other factors, not only cadherin, is also critical for cadherin dimer dissociation.

To validate the role of cadherin endocytosis in cadherin dimer dissociation, we have sought to document cadherin internalization directly in adherens junctions. Our ultrastructural analysis of A-431 cells showed that the plasma membrane invaginations resembling clathrin-coated pits are often associated with cell–cell junctions. Immuno-EM confirmed that these invaginations recruit E-cadherin. Importantly, cadherin-containing invaginations were found within a vast array of cadherin-based adhesion sites: in well-developed adherens junctions, around desmosomes, and in low-organized, perhaps very transient contacts between cell bodies and filopodia. Similar structures were also observed in the nontumorigenic HaCaT keratinocytes. The presence of E-cadherin at both the endocytic invagination and the adjoining surface of a contacting cell suggests that the internalization forces can directly fracture cadherin adhesive links. A similar process, endocytosis-driven fracture of the adhesion sites, has been proposed to facilitate cell migration. By this process the adhesion protein integrin is constantly internalized from the cell-substrate contact sites at the rear of the cell and subsequently transported to the leading edge (Palecek *et al.,* 1996).

Adherens junctions are not the unique sites for E-cadherin on the cell surface. Numerous cadherin molecules were detected at extrajunctional apical and lateral cell surfaces. In the junction-free regions cadherin appears as small isolated clusters of gold particles. Although a special study is needed to compellingly determine whether each gold cluster represents a single cadherin molecule or its lateral dimer, this

observation supports our biochemical data that only a fraction of E-cadherin molecules is involved in cell–cell contact formation.

The apical and lateral surfaces differ with respect to endocytosis: no single example of cadherin-containing coated pit-like structures has been observed on the apical cell membrane. This observation is in accordance with data reported by Paterson *et al.* (2003). This work showed that isolated epithelial cells (whose surface apparently corresponds to the apical surface of our cells) internalize E-cadherin via macropinocytosis. Taken together, these data suggest that specific signaling mechanisms determine the pathway of cadherin endocytosis at the lateral and apical surfaces. Furthermore, mechanisms underlying cadherin endocytosis within adherens junctions and at extrajunctional areas of the lateral surface might also be different. Clarifying this issue will require immuno-EM using a panel of antibodies against different endocytic markers. This work will help to understand the complexity of cadherin endocytosis and will result in better strategies for managing cadherin-based adhesion.

In conclusion, our work shows that an active cellular process is involved in the disassembly of cadherin adhesive dimers, which are remarkably strong protein complexes in vitro. The inactivation of this process by ATP depletion or by treatments inhibiting endocytosis results in the immediate stabilization of cadherin dimers and in a dramatic increase in their total amounts. The role of cadherin endocytosis is further confirmed by immuno-EM showing that E-cadherin is internalized directly from adherens junctions. Thus, cadherin endocytosis alone, or in concert with other mechanisms, controls the lifetime of cadherin adhesive dimers, thereby regulating the dynamics and plasticity of cadherin-based adhesive sites.

ACKNOWLEDGMENTS

We thank Wandy Beatty (Molecular Microbiology Imaging Facility, Washington University Medical School) for help in electron microscopy. We also thank Drs. V. Gelfand and A. Kashina for valuable discussion. This work has been supported in part by Grant AR44016-04 from the National Institutes of Health.

REFERENCES

Adams, C. L., Chen, Y. T., Smith, S. J., and Nelson, W. J. (1998). Mechanisms of epithelial cell-cell adhesion and cell compaction revealed by high-resolution tracking of E-cadherin-green fluorescent protein. J. Cell Biol. *142*, 1105–1119.

Akhtar, N., and Hotchin, N. A. (2001). RAC1 regulates adherens junctions through endocytosis of E-cadherin. Mol. Biol. Cell *12*, 847–862.

Boggon, T. J., Murray, J., Chappuis-Flament, S., Wong, E., Gumbiner, B. M., and Shapiro, L. (2002). C-cadherin ectodomain structure and implications for cell adhesion mechanisms. Science *296*, 1308–1313.

Bryant, D. M., and Stow, J. L. (2004). The ins and outs of E-cadherin trafficking. Trends Cell Biol. *14*, 427–434.

Chitaev, N. A., and Troyanovsky, S. M. (1998). Adhesive but not lateral E-cadherin complexes require calcium and catenins for their formation. J. Cell Biol. *142*, 837–846.

Cooper, J. A. (1987). Effects of cytochalasin and phalloidin on actin. J. Cell Biol. *105*, 1473–1478.

Coue, M., Brenner, S. L., Spector, I., and Korn, E. D. (1987). Inhibition of actin polymerization by latrunculin A. FEBS Lett. *213*, 316–318.

Gumbiner, B. M. (2005). Regulation of cadherin-mediated adhesion in morphogenesis. Nat. Rev. Mol. Cell. Biol. *6*, 622–634.

Heuser, J. E., and Anderson, R. G. (1989). Hypertonic media inhibit receptor-mediated endocytosis by blocking clathrin-coated pit formation. J. Cell Biol. *108*, 389–400.

Heuser, J. E. (1989). Effects of cytoplasmic acidification on clathrin lattice morphology. J. Cell Biol. *108*, 401–411.

Huen, A. C., *et al.* (2002). Intermediate filament-membrane attachments function synergistically with actin-dependent contacts to regulate intercellular adhesive strength. J. Cell Biol. *159*, 1005–1017.

Ivanov, A. I., Nusrat, A., and Parkos, C. A. (2004). Endocytosis of epithelial apical junctional proteins by a clathrin-mediated pathway into a unique storage compartment. Mol. Biol. Cell *15*, 176–188.

Ivanov, A. I., Nusrat, A., and Parkos, C. A. (2005). Endocytosis of the apical junctional complex: mechanisms and possible roles in regulation of epithelial barriers. Bioessays *27*, 356–365.

Izumi, G., Sakisaka, T., Baba, T., Tanaka, S., Morimoto, K., and Takai, Y. (2004). Endocytosis of E-cadherin regulated by Rac and Cdc42 small G proteins through IQGAP1 and actin filaments. J. Cell Biol. *166*, 237–248.

Jarrett, O., Stow, J. L., Yap, A. S., and Key, B. (2002). Dynamin-dependent endocytosis is necessary for convergent-extension movements in *Xenopus* animal cap explants. Int. J. Dev. Biol. *46*, 467–473.

Klingelhofer, J., Laur, O. Y., Troyanovsky, R. B., and Troyanovsky, S. M. (2002). Dynamic interplay between adhesive and lateral E-cadherin dimers. Mol. Cell. Biol. *22*, 7449–7458.

Kusumi, A., Suzuki, K., and Koyasako, K. (1999). Mobility and cytoskeletal interactions of cell adhesion receptors. Curr. Opin. Cell Biol. *11*, 582–590.

Laube, G., Roper, J., Pitt, J. C., Sewing, S., Kistner, U., Garner, C. C., Pongs, O., and Veh, R. W. (1996). Ultrastructural localization of Shaker-related potassium channel subunit and synapse-associated protein 90 to septate-like junctions in rat cerebellar Pinceaux. Brain Res. Mol. Brain Res. *42*, 51–61.

Laur, O. Y., Klingelhofer, J. Troyanovsky, R. B., and Troyanovsky, S. M. (2002). Both the dimerization and immunochemical properties of E-Cadherin EC1 domain depend on Trp(156) residue. Arch. Biochem. Biophys. *400*, 141–147.

Le, T. L., Yap, A. S., and Stow, J. L. (1999). Recycling of E-cadherin: a potential mechanism for regulating cadherin dynamics. J. Cell Biol. *146*, 219–232.

Leckband, D., and Sivasankar, S. (2000). Mechanism of homophilic cadherin adhesion. Curr. Opin. Cell Biol. *12*, 587–592.

Lu, Z., Ghosh, S., Wang, Z., and Hunter, T. (2003). Downregulation of caveolin-1 by EGF leads to the loss of E-cadherin, increased transcriptional activity of beta-catenin, and enhanced tumor cell invasion. Cancer Cell *4*, 499–515.

Nelson, W. J., Drees, F., and Yamada, S. (2005). Interaction of cadherin with the actin cytoskeleton. Novartis Found. Symp. *269*, 159–168.

Ozawa, M. (2002). Lateral dimerization of the E-cadherin extracellular domain is necessary but not sufficient for adhesive activity. J. Biol. Chem. *277*, 19600–19608.

Palacios, F., Schweitzer, J. K., Boshans, R. L., and D'Souza-Schorey, C. (2002). ARF6-GTP recruits Nm23–H1 to facilitate dynamin-mediated endocytosis during adherens junctions disassembly. Nat. Cell Biol. *4*, 929–936.

Palecek, S. P., Schmidt, C. E., Lauffenburger, D. A., and Horwitz, A. F. (1996). Integrin dynamics on the tail region of migrating fibroblasts. J. Cell Sci. *109*, 941–952.

Patel, S. D., Chen, C. P., Bahna, F., Honig, B., and Shapiro, L. (2003). Cadherin-mediated cell-cell adhesion: sticking together as a family. Curr. Opin. Struct. Biol. *13*, 690–698.

Paterson, A. D., Parton, R. G., Ferguson, C., Stow, J. L., and Yap, A. S. (2003). Characterization of E-cadherin endocytosis in isolated MCF-7 and chinese hamster ovary cells: the initial fate of unbound E-cadherin. J. Biol. Chem. *278*, 21050–21057.

Provost, E., and Rimm, D. L. (1999). Controversies at the cytoplasmic face of the cadherin-based adhesion complex. Curr. Opin. Cell Biol. *11*, 567–573.

Shan, W. -S., Tanaka, H., Phillips, G. R., Arndt, K., Yoshida, M., Colman, D. R., and Shapiro, L. (2000). Functional cis-heterodimers of N- and R-cadherins. J. Cell Biol. *148*, 579–590.

Shapiro, L., *et al.* (1995). Structural basis of cell-cell adhesion by cadherins. Nature *374*, 327–337.

Shelden, E. A., Weinberg, J. M., Sorenson, D. R., Edwards, C. A., and Pollock, F. M. (2002). Site-specific alteration of actin assembly visualized in living renal epithelial cells during ATP depletion. J. Am. Soc. Nephrol. *13*, 2667–2680.

Troyanovsky, S. M. (2005). Cadherin dimers in cell-cell adhesion. Eur. J. Cell Biol. *84*, 225–233.

Troyanovsky, R. B., Sokolov, E., and Troyanovsky, S. M. (2003). Adhesive and Lateral E-cadherin dimers are mediated by the same interface. Mol. Cell. Biol. *23*, 7965–7972.

Vasioukhin, V., Bauer, C., Yin, M., and Fuchs, E. (2000). Directed actin polymerization is the driving force for epithelial cell-cell adhesion. Cell *100*, 209–219.